ARTICLES

Crystallization and Colloidal Stability of Calcium Phosphate Phases

Yue Liu and George H. Nancollas*

Department of Chemistry, State University of New York at Buffalo, Buffalo, New York 14260

Received: August 8, 1996; In Final Form: January 14, 1997[⊗]

The interfacial energy of calcium phosphate powders has been determined through contact angle measurements using thin-layer wicking techniques. The much smaller interfacial energy of octacalcium phosphate (OCP) in contact with water compared with that of hydroxyapatite (HAP) supports the observation that the crystallization of the latter may be preceded by an OCP phase which can serve as a template for apatite growth. The colloidal stabilities of calcium phosphates of colloidal dimensions were also investigated. The relative stabilities of OCP, dicalcium phosphate dihydrate (DCPD), and HAP dispersions could be explained by invoking the concepts of Lewis acid−base interactions in addition to the two other more traditional types of interactions that are involved in the Derjaguin−Landau−Verwey−Overbeek (DLVO) theory, namely, electrical double-layer repulsion and van der Waals attraction.

Introduction

The concept of surface energy was first used to explain crystal growth by Curie in 1885.[1] In this theory, it was proposed that, during the growth of a crystal, the total surface energy contributed by all the faces of the crystal was at a minimum. Wulff[2] extended the surface energy theory, suggesting, from measurements of the growth velocities of crystals of Mohs' salt, that the crystal faces would grow at rates proportional to their respective surface energies. There is little experimental evidence to support these early surface energy theories of crystal growth, mainly because the surface energy of a crystal is important only when the dimensions are in the micron range. The "equilibrium shape" is never observed with macroscopic crystals (in the millimeter range); their shape is determined by the kinetics of the growth processes, which are usually anisotropic. In addition, the most serious defect of these theories was their inability to interpret the influence of supersaturation on the rates of crystal growth. For these reasons, surface energy theories of crystal growth were virtually abandoned. However, the concept of surface energy did not disappear; it entered into the picture of nucleation as an important parameter. The interfacial energy between a precipitate particle (or a nucleus) and the surrounding medium is also a critical parameter in reconciling experimental data with nucleation theory. Classical theories of homogeneous nucleation have been successful for the nucleation of liquid droplets from vapor and for crystal formation in melts.[3−5] In all these cases the interfacial energies could be calculated from the nucleation data by means of the theory of nucleation and compared with estimates from macroscopic equilibrium measurements.

In biological systems, calcium phosphate mineralization has frequently been suggested as proceeding through precursor phases such as amorphous calcium phosphate (ACP) or octacalcium phosphate (OCP) before transformation to the thermodynamically more stable hydroxyapatite (HAP).[6−8] In the present study, these observations are expounded in physicochemical terms by considering the differences in surface properties of various calcium phosphate phases.

One of the most important physical properties of small particle dispersions is the tendency for aggregation. Yet, this aspect of biomineralization has been little studied. It has been suggested that aggregation and dispersion of hydroxyapatite crystallites may be important in the formation and destruction of calcified tissues and may contribute to their structural strength and hardness.[9] Aggregation may also play a role in pathological conditions such as ectopic calcification and dental calculus. In the case of urinary stones, aggregation has been suggested as a predominant factor during calcium oxalate formation in urolithiasis.[9] In this paper, the relative stability of OCP, DCPD, and HAP dispersions is discussed by invoking the concepts of Lewis acid−base interactions in addition to the two other more traditional types of interactions that are involved in the Derjaguin−Landau−Verwey−Overbeek (DLVO) theory: electrical double-layer repulsion and van der Waals attraction.

Experimental Section

HAP was prepared by the dropwise addition of 2.0 L of a solution of 0.15 mol L^{-1} $H(NH_4)_2PO_4$ and 5.7% (1.5 mol L^{-1}) NH_4OH to 7.0 L of a solution 0.08 mol L^{-1} Ca $(NO_3)_2$ and 0.8% (0.2 mol L^{-1}) NH_4OH. Following the addition, which was completed in 5 h, 0.06 L of 28% NH_4OH was added and the suspension was refluxed at pH 10 for 12 h. After filtration, the solid was washed twice with 2 L of triply distilled water (TDW) and dried at 140 °C; the Ca/P molar ratio was 1.66 ± 0.02. OCP was prepared using a method similar to that of LeGeros.[10] To 0.25 L of 0.02 mol L^{-1} sodium phosphate solution (pH 5) was added 0.25 L of 0.02 mol L^{-1} calcium acetate solution dropwise over a period of 3−4 h at a temperature of 60 °C. The Ca/P molar ratio was 1.33 ± 0.02. DCPD, obtained from Aldrich Chemical Co., had a Ca/P molar ratio of 1.02 ± 0.02. The crystals were analyzed using X-ray powder diffraction (Siemens Nicolet/Nic spectrometer, Cu Kα radiation with a Ni filter, position sensitive detector in the transmission mode, and STOE attachments) and FTIR, which showed peaks characteristic of the respective crystalline phases.

Interfacial energies were obtained by a thin-layer wicking method,[11] based on the Washburn equation (eq 1),[12] relating

[⊗] Abstract published in *Advance ACS Abstracts,* April 15, 1997.

S1089-5647(96)02403-0 CCC: $14.00

contact angles of the liquid formed on the solid surfaces to the rate of penetration of liquids through the powdered substrate (see also Ku *et al.*[13])

$$h^2 = \frac{tR\gamma_L \cos\theta}{2\eta} \quad (1)$$

In eq 1, R is the effective interstitial pore radius, γ_L, the surface tension, θ, the contact angle of the liquid on the solid, η, the viscosity of the liquid, and h, the length the liquid column moved in a given time t. For the determination of contact angles, the value of R in eq 1 must be ascertained independently. This can be done by calibration involving low-energy apolar liquids, usually alkanes such as heptane, octane, decane, dodecane, and hexadecane, which spread over the solid surface without forming a finite contact angle. It has been shown[11] that with such spreading liquids, θ remains exactly at zero, so that eq 1 can be solved for R. With a knowledge of R, the contact angles between the solid and the test liquids α-bromonaphthalene, diiodomethane, water, ethylene glycol, and formamide can be determined.

It is should be emphasized that contact angles measured by thin-layer wicking are not those formed by liquids on the exterior surfaces of a solid support fabricated from powders. The latter are rough, and hysteresis effects would be severe. Instead of the exterior surfaces of powder blocks, a model involving the network of irregular channels of a thin layer of the powder material is used. In applying the Washburn equation, the actual network of irregular channels is replaced by a bundle of cylindrical pores of radius R. In view of the approximate nature of this model, the Laplace equation is used to derive the Washburn equation. Thus, the contact angles as obtained by thin-layer wicking are those formed by the liquids with the walls of the channels. With monosized cuboid hematite particles, which on account of their shape allowed direct contact angle measurement, as well as contact angle determination by thin-layer wicking, essentially the same contact angles were obtained with the same apolar and polar contact angle liquids.[14]

To prepare thin layers for contact angle measurements, 1.5 wt % suspensions of HAP, OCP, and DCPD crystallite particles in distilled water or ethyl alcohol were made. These were maintained in homogeneous suspension by continuous magnetic stirring, and 5 mL aliquots were withdrawn by pipet and evenly distributed on clean horizontal glass microscope slides (7.5 cm × 2.5 cm). The liquid phase was allowed to evaporate at room temperature for several hours before drying overnight in an oven at 105 °C and storing in a desiccator. Before use in wicking experiments, indentations were made at intervals of 2.0 mm on the powder coating of each slide beginning about 5 mm from the end of the slide to be immersed in the liquids.

The actual thin-layer wicking was done by placing the dried, coated glass slides in containers with gas-tight rubber stoppers with slots to accommodate the slides. Different glass containers were filled to a height of about 5 mm with one of the various liquids listed in Table 1.[11] Before immersing the tips of the coated slides into the liquids, they were kept inside the closed glass containers for about 1 h to equilibrate the powders with the vapors of the low energy-spreading liquids (alkanes). No equilibration was necessary with the test liquids: α-bromonaphthalene, diiodomethane, water, ethylene glycol, and formamide. After equilibration, the slides were immersed in the liquids to a liquid height of about 5 mm, and the rates of vertical movement of the liquid fronts through the layers of powder were measured for several timed events. Approximately 35 slides were prepared using each powder, and each liquid test was made with at least three slides. It should be noted that for nonspreading liquids, prolonged exposure of the powders to the liquid vapors did not influence the calculated contact angles. These vapors of the nonspreading liquids did not deposit on the solid surfaces.[11]

TABLE 1: Values of the Surface Tension Components and Parameters (mJ m^{-2}) and of the Viscosity (poise) of Wicking Liquids Used for Contact Angle Measurements (20 °C)

liquid	γ_L	γ_L^{LW}	γ_L^+	γ_L^-	η
heptane	20.1	20.1	0	0	0.00409
octane	21.6	21.6	0	0	0.00542
decane	23.8	23.8	0	0	0.00907
dodecane	25.35	25.35	0	0	0.01493
hexadecane	27.5	27.5	0	0	0.03
α-bromonaphthalene	44.4	44.4	≈0	≈0	0.0489
diiodomethane	50.8	50.8	≈0	≈0	0.028
ethylene glycol	48.0	29.0	1.92	47.0	0.199
formamide	58.0	39.0	2.28	39.6	0.0455
water	72.8	21.8	25.5	25.5	0.010

TABLE 2: The Interfacial Energy Components and Parameters (mJ m^{-2}) As Determined by Thin-Layer Wicking at 20 °C

material	γ_s	γ_s^{LW}	γ_s^+	γ_s^-	γ_{sw}
HAP	36.2	28.5	0.92	16.0	9.0
OCP	34.7	21.6	2.19	19.7	4.3
DCPD	40.4	26.4	1.55	31.7	−4.2

Results and Discussions

Crystallization and Surface Energy of Calcium Phosphates. Calculations of the interfacial energy terms from the measured contact angle were based on Young's equation adapted for polar systems[15] and contact angle values from Table 1:

$$\gamma_L(1 + \cos\theta) = 2(\sqrt{\gamma_S^{LW}\gamma_L^{LW}} + \sqrt{\gamma_S^+\gamma_L^-} + \sqrt{\gamma_S^-\gamma_L^+}) \quad (2)$$

where γ_S^{LW} is the Lifshitz−van der Waals (LW) component of the surface energy of the solid and γ^+ and γ^- are the Lewis acid and base surface energy parameters, respectively. The results are summarized in Table 2 in which γ_s is the surface energy of the solid (against air or its vapor), γ_{sw} the interfacial energy of the solid against water, γ_s^{LW} the Lifshitz−van der Waals component of γ_s, and γ_s^+ and γ_s^- are the Lewis acid and base parameters for γ_s. The surface tension values in Table 2 compare favorably with available literature values. Thus Christoffersen reported an interfacial energy of 45 mJ m^{-2} for HAP from crystal growth and dissolution experiments. Using contact angle measurements on single crystals, Busscher gave values of 39 and 30 mJ m^{-2} for basal and prismatic planes of HAP, respectively. The discrepancies may in part arise from the fact that different experimental methods may yield different energetic parameters. The values from thin-layer wicking are averages over the crystal faces.

Of the several commonly encountered calcium phosphate phases, HAP is thermodynamically the most stable and is usually assumed to be a model structural component for biological mineral phases. However, there is little doubt that other phases, such as dicalcium phosphate dihydrate (DCPD), dicalcium phosphate (DCPA), octacalcium phosphate (OCP), and β-tricalcium phosphate (β-TCP), may also participate in the crystallization reaction. Crystallization of many sparingly soluble salts probably involves the formation of metastable precursor phases which subsequently dissolve and transform as the precipitation reaction proceeds. Clear evidence for the formation of OCP as an intermediate in the precipitation of HAP was also obtained by Meyer and Eanes.[16] In determining the likelihood of the formation of intermediate crystal phases in solutions supersatu-

rated with respect to several different minerals, kinetic factors are important. Thus the formation of HAP is much slower than that of either OCP or DCPD under equivalent thermodynamical driving forces, and during the precipitation reactions larger proportions of the kinetically favored phase may be observed. The balance between kinetic and thermodynamic factor is, therefore, very important in discussing the likelihood of precursor formation during calcium phosphate precipitation.

The roles of OCP and DCPD as calcium phosphate precipitation precursors have been investigated from a physicochemical point of view by studying their surface energies. For small crystals (in the micron range), surface energy plays an important role in determining both the kinetics of formation and their "equilibrium shape". In terms of the classical nucleation theory, the Gibbs free energy of formation of a critical nucleus is proportional to the third power of the interfacial energy for both the homogeneous (eq 3),

$$\Delta G^* = \frac{16\pi}{3}\frac{\gamma^3}{(\Delta G_v)^2} \tag{3}$$

and heterogeneous (eq 4) nucleation reactions

$$\Delta G^*_{\text{het}} = \frac{16\pi}{3}\frac{\gamma_{\alpha\beta}{}^3}{(\Delta G_v)^2}\frac{(1-\cos\theta)^2(2+\cos\theta)}{4} = \frac{16\pi}{3}\frac{\gamma\alpha\beta^3}{(\Delta G_v)^2}\phi \tag{4}$$

For homogeneous nucleation, the Gibbs free energy barrier for the formation of a critical nucleus may be approximated as eq 5

$$\Delta G^* \propto \frac{\gamma^3}{(\ln S)^2} \tag{5}$$

where S is the supersaturation ratio with respect to the precipitating phase and γ is the interfacial energy between the precipitate and the medium. Ignoring the differences between the molar volumes of HAP ($Ca_5(PO_4)_3OH$) and OCP ($Ca_4H(PO_4)_3 \cdot 2.5H_2O$), eq 5 can be applied to each of these phases. When the supersaturation ratios are the same, the rate of nucleation depends strongly on the interfacial energy terms (eq 3). The interfacial energy of HAP against water is more than twice as large as that of OCP (Table 2), so the activation energy of HAP would be about 10 times that of OCP. OCP would, therefore, be expected to nucleate at a much faster rate than HAP.

However, in most cases, the solution supersaturation ratios are not the same with respect to both HAP and OCP, so the conclusions reached above are not applicable. For example, a solution having a certain supersaturation ratio with respect to HAP usually does not have the same OCP supersaturation ratio due to differences in solubility products. In fact, a solution supersaturated with respect to HAP can be undersaturated with respect to OCP. For example, a solution prepared at 37 °C with $[CaCl_2] = 0.40 \times 10^{-3}$ mol L^{-1} and $[KH_2PO_4] = 0.24 \times 10^{-3}$ mol L^{-1}, with pH adjusted to 7.4 and ionic strength of 0.15 mol L^{-1}, would be supersaturated with respect to HAP ($\sigma_{HAP} = 3.6$) and undersaturated with respect to OCP ($\sigma_{OCP} = -0.18$). Using eq 5, along with the interfacial energy values for HAP and OCP (Table 2), it can be shown that when

$$S_{OCP} > (S_{HAP})^{0.33} \tag{6}$$

where S_{OCP} and S_{HAP} are the solution supersaturation ratios with respect to OCP and HAP, respectively, the rate of nucleation of OCP will be faster than that of HAP. In other words, OCP will appear before the thermodynamically more stable HAP, even though the solution is more supersaturated with respect to the latter. In terms of relative supersaturations, eq 6 can also be written as eq 7

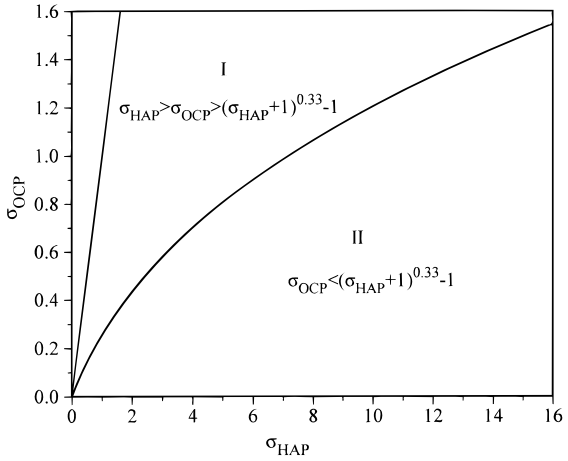

Figure 1. Graphic representation of calcium phosphate solutions supersaturated with respect to OCP and HAP showing regions of different rates of nucleation of OCP and HAP.

$$\sigma_{OCP} > (\sigma_{HAP} + 1)^{0.33} - 1 \tag{7}$$

and represented graphically in Figure 1. In region I, where eq 7 is satisfied, OCP is expected to precipitate more readily than HAP, while in region II, nucleation of HAP is both thermodynamically and kinetically favored over OCP. In order to test this hypothesis, solutions that fall in region I were prepared at 37 °C with $[CaCl_2] = 4.77 \times 10^{-3}$ mol L^{-1} and $[KH_2PO_4] = 3.56 \times 10^{-3}$ mol L^{-1}. The pH was adjusted to 6.0 and the ionic strength to 0.08 mol L^{-1}. The relative supersaturation with respect to HAP is $\sigma_{HAP} = 5.3$ and OCP, $\sigma_{OCP} = 0.90$. Under these conditions, the exclusive growth of OCP was observed in constant composition growth experiments.[17]

Using surface tension components and parameters from Table 2 and eq 8,[11]

$$\gamma_{12} = (\sqrt{\gamma_1^{LW}} - \sqrt{\gamma_2^{LW}})^2 + 2(\sqrt{\gamma_1^+\gamma_1^-} + \sqrt{\gamma_2^+\gamma_2^-} - \sqrt{\gamma_1^+\gamma_2^-} - \sqrt{\gamma_1^-\gamma_2^+}) \tag{8}$$

an interfacial energy between HAP and OCP, $\gamma_{HAP,OCP}$, of 0.93 mJ m^{-2} was evaluated.[18] The angle of contact between the HAP deposit and the OCP surface, θ, corresponding to the angle of wetting in liquid−solid systems, was calculated as $\theta = 67.7°$ using Young's equation. The value of the factor ϕ in eq 4 was 0.23, implying that the energy barrier for the nucleation of HAP is reduced by a factor of 0.23 on OCP as compared to the homogeneous nucleation of HAP and that the nucleation of HAP was much faster at OCP surfaces. These results suggest that, under physiological conditions, OCP is likely to provide a scaffold for HAP nucleation and will precipitate first.

Colloidal Stability. In general, the stability of colloidal systems may be understood in terms of DLVO theory,[19,20] which takes into account the electrostatic (EL) and the Lifshitz−van der Waals electrodynamic (LW) interactions between particles. It involves estimations of the energy due to the overlap of electric double layers (usually repulsive) and the van der Waals

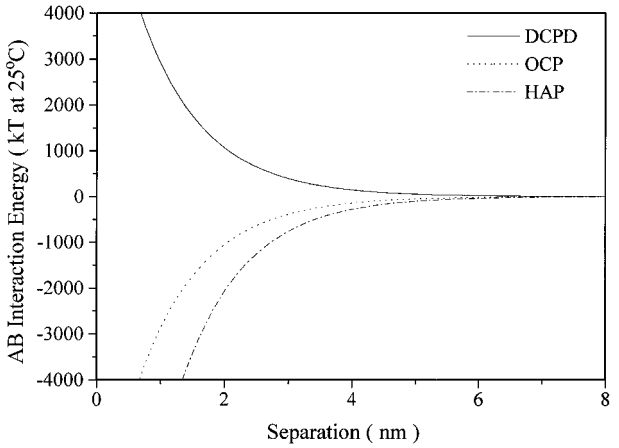

Figure 2. AB interaction energy between particles ($R = 1$ μm) of DCPD, OCP, and HAP in aqueous medium.

energy (usually attractive) in terms of interparticle distance. Colloidal stability is then interpreted in terms of the nature of the energy−distance curves. However, interactions other than EL and LW exist between surfaces in liquids.[21] It was suggested that the origin of these forces lies in electron acceptor−electron donor interactions (in the Lewis acid−base, AB, sense).[15,22] The contributions of the AB interaction to the total surface energy can be determined through contact angle measurements. For two spheres of radius R, the mode of dependency of AB interaction on separation is given by eq 9,[23]

$$\Phi^{AB} = -\pi R\lambda\Delta G^{AB} \exp\left[\frac{d_0 - d}{\lambda}\right] \qquad (9)$$

where ΔG^{AB} is the AB interaction energy per unit area between two parallel, flat surfaces in the same medium, at the minimum equilibrium separation d_0 ($d_0 = 1.57$ Å). In water, $\Delta G^{AB} = -2\gamma_{sw}^{AB}$. λ is the decay length of the liquid molecules ($\lambda = 10$ Å for water).

The AB interaction energy in water is plotted as a function of interparticle distance in Figure 2 for DCPD, OCP, and HAP having particle radii of $R = 1$ μm. It can be seen that the values for OCP and HAP are negative, while that for DCPD is positive at all separations. When the AB interaction predominates over the EL and LW interactions, OCP and HAP tend to flocculate rapidly, while DCPD, due to the repulsive AB interaction, will tend to remain dispersed thermodynamically. Unlike the double-layer interaction, the AB interaction potentials are largely insensitive to variations in electrolyte concentration and pH.

Three suspensions (1 wt %) of DCPD, OCP, and HAP with average particle sizes for DCPD, OCP, and HAP, 9.3, 11.2 and 8.0 μm, respectively, were prepared in 0.1 mol L^{-1} NaCl solutions. Figure 3 shows photographs taken about 24 h after the preparation. It can be seen that all the dispersions collapsed with the exception of DCPD, which remained stable for more than 2 days. The fact that the dispersion behavior of these calcium phosphates could be explained by considering only the AB interaction is an indication that, in polar and especially in aqueous solutions, AB energies, whether repulsive or attractive, commonly are much more important than LW and EL interactions at smaller separations. Indeed, as demonstrated in Figure 4, where the total interaction energies including EL, LW, and AB forces are plotted for DCPD, OCP, and HAP, the same conclusions regarding their dispersion behavior can be drawn. It should be noted that the curves in Figure 2 closely resemble those in Figure 4, which indicates that in all three cases AB forces are the predominant ones.

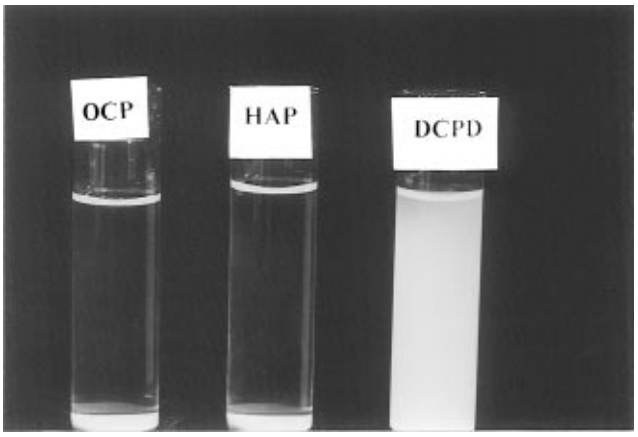

Figure 3. Suspensions of HAP, OCP, and DCPD in 0.1 mol L^{-1} NaCl solutions.

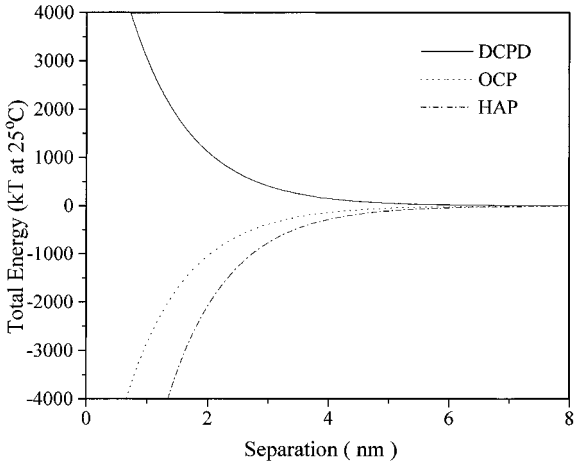

Figure 4. Total interaction energy (EL + LW + AB) between particles ($R = 1$ μm) of DCPD, OCP, and HAP in aqueous medium. The ζ-potentials are −12.13, 5.12, and −4.59 mV for DCPD, OCP, and HAP, respectively, at pH = 7.4 and 0.1 mol L^{-1} ionic strength.

The critical parameter that accounts for the different behavior of DCPD was γ_s^-, the electron-pair-donating parameter of the surface (Table 2). This was much greater for DCPD than for OCP and HAP, indicating that the DCPD surface is hydrophilic whereas OCP and HAP are hydrophobic.[24] The hydrophilicity may have resulted from its crystal structure, which consists of chains of $CaPO_4$ arranged parallel to each other[25] with lattice water molecules interlayered between the calcium and phosphate chains. The higher value of γ_s^- for DCPD was also responsible for the negative interfacial energy against water (Table 2), which is normally associated with thermodynamically unstable interfaces.[23] Such a system will tend to spontaneously relax by either abolishing the interface or by reverting to a more stable geometric configuration, ultimately resulting in zero interfacial energy.

The strongly asymmetric AB forces with high γ_s^- are responsible for the orientation of water molecules adsorbed on the surfaces of the material. Water molecules oriented on the surface of one particle will repel those oriented in the same manner on the surface of an adjacent particle.[26] If the orientation of the water molecules by the particle surface is sufficiently strong, the two particles will not be able to approach each other. On the other hand, if the AB forces are less asymmetric, the adsorbed water molecules will be less oriented and the particles will approach each other under the influence of their net van der Waals attraction.

Acknowledgment. We thank the National Institutes of Health (Grant DE03223) for support of this work.

References and Notes

(1) Curie, P. *Bull. Soc. fr. Minér.* **1885**, *8*, 145.
(2) Wulff, G. *Z. Krist.* **1901**, *34*, 449.
(3) Walton, A. G. *The Formation and Properties of Precipitates*, Interscience: New York, 1967.
(4) Zettlemoyer, A. C. *Nucleation*, Dekker: New York, 1970.
(5) Nielsen, A. E.; Sarig, S. *J. Cryst. Growth* **1971**, *8*, 1.
(6) Christoffersen, J.; Christoffersen, M. R.; Kiblczyc, W.; Andersen, F. A. *J. Cryst. Growth* **1989**, *94*, 767.
(7) Tomazic, B. B.; Tung, T. S.; Gregory, T. M.; Brown, W. E. *Scanning Mic*rosc. **1989**, *3*, 119.
(8) Meyer, J. L; Eanes, E. D. *Calcif. Tiss. Res.* **1978**, *25*, 209.
(9) Hansen, N. M.; Felix, R.; Bisaz, S.; Fleisch, H. *Biochem. Biophys. Acta* **1976**, *451*, 549.
(10) LeGeros, R. Z. *Calcif. Tissue Int.* **1985**, *37*, 194.
(11) van Oss, C. J.; Giese, R. F.; Li, Z.; Murphy, K.; Norris, J.; Chaudhury, M. K.; Good, R. J. *J. Adhesion Sci. Technol.* **1992**, *6*, 413.
(12) Washburn, E. W. *Phys. Rev.* **1921**, *17*, 273.
(13) Ku, C. A.; Henry, J. D.; Siriwardane, R.; Roberts, L. *J. Colloid Interface Sci.* **1985**, *106*, 377.
(14) Costanzo, P. M.; Wu, W.; Giese, R. F.; van Oss, C. J. *Langmuir* **1995**, *11*, 1827.
(15) van Oss, C. J.; Chaudhury, M. K.; Good, R. J. *Chem. Rev.* **1988**, *88*, 927.
(16) Meyer, J. L.; Eanes, E. D. *Calcif. Tiss. Res.* **1978**, *25*, 209.
(17) Heughebaert, J. C.; Nancollas, G. H. *J. Phys. Chem.* **1984**, *88*, 2478.
(18) Liu, Y.; Wu, W.; Sethuraman, G.; Nancollas, G. H. *J. Crystal Growth*, in press.
(19) Derjaguin, B. V.; Landau, L. D. *Acta Physicochim. URSS* **1941**, *14*, 633.
(20) Verwey, E. J. W.; Overbeek, J. Th.G. *Theory of the Stability of Lyophobic Colloids*; Elsevier: Amsterdam, 1948.
(21) Israelachvili, J. N.; McGuiggan, P. M. *Science* **1988**, *241*, 795.
(22) van Oss, C. J.; Chaudhury, M. K.; Good, R. J. *Advan. Colloid Interface Sci.* **1987**, *28*, 35.
(23) van Oss, C. J. *Interfacial Forces in Aqueous Media*; Dekker: New York, 1994.
(24) van Oss, C. J.; Giese, R. F. *Clays Minerals*, **1995**, *43*, 474.
(25) Young, R. A.; Brown, W. E. In *Biological Mineralization and Demineralization;* Nancollas, G. H., Ed.; Springer-Verlag: Berlin, 1982; pp. 101−104.
(26) Parsegian, V. A.; Rand, R. P.; Rau, D. C. *Chem. Scripta* **1985**, *25*, 28.